AN IMPROVED CROSS VENTILATION MODEL IN WINDY REGIONS

Ahmed A.Rizk, Professor
Architectural Engineering Department, Tanta University, Egypt
Yasser. A.Al- Samadony, Assistant Professor
Mechanical Power Engineering Department, Tanta University, Egypt
Usama. A.kunbr, Assistant Professor
Mustafa.M.Elwan, Assistant Professor
Architectural Engineering Department, Tanta University, Egypt

Abstract

This study suggests a new simulated model to improve cross ventilation performance inside a single room space in the different wind velocity regions. The architectural design decisions of indoor openings and walls can achieve the stagnation and the Venturi conditions that can govern the indoor air velocities inside an indoor room space to be decreased in high wind velocity regions and to be increased in low wind velocity regions. Stagnation condition occurrence when an indoor wall faces an inlet opening can decrease indoor air velocities inside a single room space with a high indoor covered ventilation area because the spreading air mass movements have the curve shapes of the contour lines that indicate ratios of the outdoor wind velocity. Venturi condition occurrence when an inlet opening faces an outlet opening can increase indoor air velocities through the openings inside single room space with the high air flow rates because the penetrating air mass movements have the spire shapes of the contour lines that indicate ratios of the outdoor wind velocity. Hurghada City, Egypt, is selected as an example of windy regions while a single room space is selected as an example of indoor spaces for field and simulation experiments.

Keywords: Cross ventilation; Thermal comfort; Computational fluid dynamics

Introduction

Ventilation of indoor spaces is the best way to achieve thermal comfort in the different windy regions. The study focuses on how to apply cross ventilation by a driven wind.

Two approaches can achieve thermal comfort inside an indoor space. The first approach uses direct cooling depended on the spread of indoor air mass movements to cover a higher ventilation area with an acceptable air velocity. The second approach uses indirect cooling depended on the penetration of indoor air mass movements to increase air velocity through the openings with the increase of air flow rates. The first approach can be applied when the outdoor wind temperature is or less than 26°C; where the air flow patterns are not required to be well distributed, Givoni [1]. The second approach extends thermal comfort up to 32°C, Borger et al [2], Givoni [3], Olgyay [4] and ASHRAE [5]; where the air flow patterns are required to be well distributed. Thermal comfort can be achieved up to 35°C if the air flow patterns cover the highest ventilation area, Karava et al [6]. The mathematical and the positional relationships between inlet openings and outlet openings can improve indoor air flow patterns, Givoni' [1] , [3] and Abdin [7]. Anderson [8] dealt with the relationships between the openings and the walls. Allard [9] focused on the effect of the perpendicular angle of wind direction through inlet openings on indoor air velocities. Mass [10] presented the effect of out wind velocity on indoor air flow patterns.

The only way to increase indoor air velocities despite a weak wind is by the Venturi effect that can be achieved through the narrow widths of openings. The only way to decrease indoor air velocities despite a strong wind is by the stagnation effect that can be achieved by the walls facing inlet openings.

Description of field and simulation experiments

Description of field experiments

An indoor single room space located in Hurghada City, Egypt, is chosen as the model case study. Table (1) presents daily outdoor wind conditions in the hot times of Hurghada City.

The model dimensions are shown in Figure (1). The model has one inlet opening and two outlet openings. One of the outlet openings faces the inlet opening. The model consists of three external walls oriented to 330° to the north having an inlet opening with different widths oriented to 330º to the North and two outlet openings with fixed widths oriented 30º to the South As shown in Figure (1). Table 2 presents the description of indoor room space models.

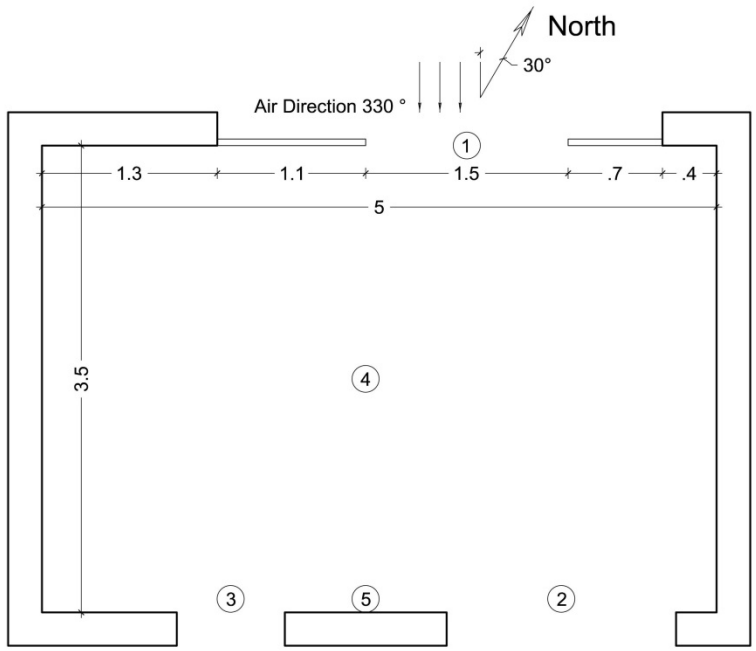

Figure (1): Experimental indoor room space model with the governing points

Table 1: Outdoor wind conditions at Hurghada City in September 2013,[11] and [12]

Wind conditions in September		**Actual solar time**											
		0 am	2 am	4 am	6 am	8 am	10 am	12 noon	2 pm	4 pm	6 pm	8 pm	10 pm
Solar air temperature ºC		30.6	29.2	28.4	27.6	31.6	36.44	38.24	39.44	39.44	35.89	32	31
Wind Velocity	**direction º**	320	330	300	330	350	340	350	350	350	340	330	310
	Velocity m/s	5	8	6	6	8	10	11	9	9	6	6.5	5
Humidity %		44	56	54	49	49	49	46	41	38	42	44	44

Table 2: Description of the experimental Indoor room space model

Model dimensions			**characteristics of the model's openings**					
Width is perpendicular to wind direction (m)	Length is along parallel wind direction (m)	Total model area (m^2)	Ratio of inlet opening width to the total width	Ratio of inlet opening area due to the total area	Ratio of inlet opening width to outlet opening widths	Position of inlet opening due to width	Position of outlet opening due to inlet opening	Notes
5	3.5	17.5	1:3	25 %	2:3 primary 1:3 secondary	At the center of width	Outlet opening facing inlet opening	The model contains two outlet openings

The first three governing points are chosen at the openings to measure the Venturi effect while the other two points are chosen in the middle of the room space and at the facing wall to measure the stagnation effect as shown in Figure (1).

Four continuous lines express the percentages of outdoor wind velocities 80%, 60%, 40% and 20% respectively obtained by measuring an indoor points on a horizontal plane grid 1 m by 1 m at a level 1.1 m along three lines and across five lines.

Portable ambient weather device WM4 is used to measure outdoor wind conditions. Air velocity is measured by means of an anemometer with a range of (0 m/s-30 m/s) and an accuracy of (± 0.1). Air temperature and air humidity are measured by using USB data logger with a range of (0 C°-120° C) and an accuracy of (± 0.1) for temperature and with a range of (0 %-100%) and an accuracy of (± 1%) for humidity while a portable indoor device Testo 410 is used to measure indoor conditions.

Three architectural case studies present the effect of the architectural design decisions related to the mathematical and the positional relationships between inlet and outlet openings in the first field experiment, the width ratios of inlet to outlet openings are 2:3 in the architectural case study no.1 and 1:3 in the architectural case studies no.2 and no.3 as shown in Figure (2). While four velocity case studies present the effect of outdoor wind velocities range from 4 m/s to 7 m/s on indoor room space air velocities. All case studies are of 30°C air temperature and of 50% relative humidity in the second field experiment.

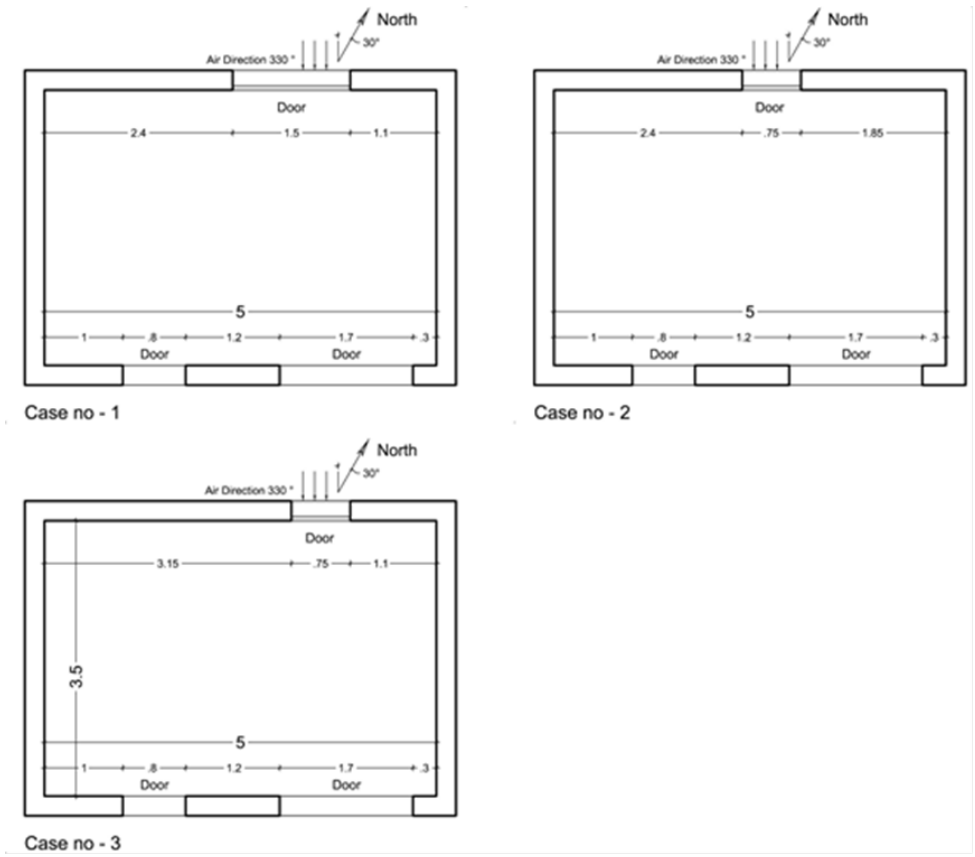

Figure (2): Different case studies due to ratios of inlet to outlet opening widths inside the experimental indoor room space model

SIMULATION EXPERIMENTS

A computational fluid dynamics software package program (ANSYS) is used to simulate the model.

The model external walls construction is of 200 mm thick light-colored heavy concrete blocks coated with 16 mm plaster (U=2.73 W/m^2 ºC) while the roof construction is of 100 mm flat reinforced concrete slab with 50 mm rigid insulation (U=0.51 W /m^2 ºC). All thermal loads are calculated on 23rd September and added to the software package program as heat fluxes. The model geometry is assumed to be a three dimensional domain. The mesh properties are three tetrahedral type layers with 229295 elements and 39029 nodes. The working fluid is air. K-Epsilon turbulence model is selected. The simulation assumes a steady state condition. The software package program uses continuity, momentum and energy equations to obtain air mass behavior inside the indoor room space and at the outlet openings with a root mean square residual error target of 10^{-4}. Inlet air conditions are assumed continuous with a uniform velocity and a uniform temperature. The

values of inlet outdoor wind velocity range from 4m/s to 7m/s, indoor air temperature (30ºC) and indoor relative humidity (50%) are fed to the software package program. The outlet openings are set at an atmospheric pressure. Domain walls are assumed smooth with a uniform heat flux per unit area of value depends on the orientation and the month. The walls, the roof and the floor heat fluxes are 2.53, 5.81, 6.28, 5.34, 10.18 and 2.11 W/m2 respectively.

In numerical outputs, the convergence was achieved as a root mean square residual error target of 10^{-4}. Velocity contours at any section inside the domain could be obtained from CFX post. Moreover, the CFX post probe may be used to know the values of air properties at any point inside the domain.

Seven governing points inside the indoor room space model are measured as in simulation experiments as shown in Figure (3).

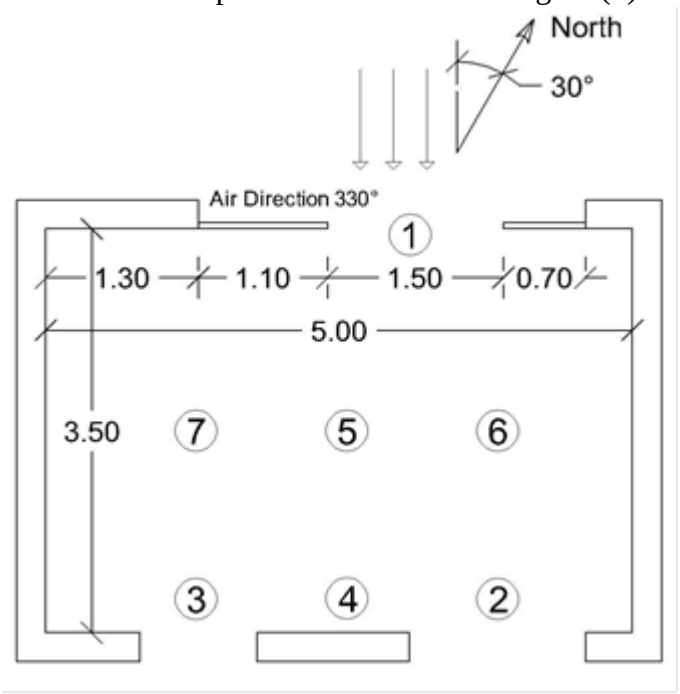

Figure (3) Simulated indoor room space model with the governing points

Two architectural case studies present the effect of the architectural design decisions as shown in Figure (2) while three velocity case studies present the effect of the outdoor wind velocity on indoor air velocities inside the indoor room space model.

The evaluation scales of field and simulation experiments are based on thermal comfort in indoor conditions. Table (3) presents the index of thermal comfort of the integrated indoor conditions. The upper limit of indoor air temperature 37°C requires an indoor air velocity 3 m/s and an

indoor relative humidity 20% meanwhile the lower limit of indoor air temperature 26°C requires an indoor air velocity 0.5 m/s and an indoor relative humidity up to 80%.

Table (3) Index of thermal comfort of the integrated indoor conditions

Air velocity m/s	**0.2**		**0.5**		**1**		**1.5**		**2**		**3**	
Relative humidity %	80	50	80	50	80	50	80	50	80	50	80	50
Air temperature C^O	27	29	29	31	30	32	32	34	33	36	34	37

Field and simulation results

Field results

Figures (4) and (5) present contour lines, each of which represents a different percentage of outdoor wind velocity. Each Figure consists of four contour lines indicate 20%, 40%, 60% and 80% of outdoor wind velocity. Tables (4) and (5) present the indoor air velocity values at the governing points.

Effect of the ratio of inlet to outlet opening widths on cross ventilation

Three models are experimented as shown in Figure (4) and Table (4). The first model shows the ratio of inlet to outlet opening widths 2:3. The other two models show the ratio of inlet to outlet opening widths 1:3. The inlet opening faces the wall in case study no-2 while the inlet opening faces the outlet opening in case study no-3. The architectural case study-1 achieves an average indoor air velocity 1.2 m/s (20% of outdoor wind velocity) or over covering a ventilation area 65% of the total room space area; the architectural case study-2 achieves the same value of indoor air velocity in a covered ventilation area 70% while the architectural case study-3 achieves a covered ventilation area 55% for the same value of indoor air velocity. Case study-1 then case study-3 are the favorable conditions in low outdoor wind velocity regions resulted from the Venturi effect at points (1) and (2), meanwhile case study-2 is the favorable condition in high outdoor wind velocity regions resulted from the stagnation effect at points (4) and (5). The spire shapes of the contour lines shown in case studies 1 and 3 can be applied only when the outdoor wind temperature is or less than 28°C, meanwhile the curve shapes of the contour lines shown in case study-2 can be applied in all conditions when the outdoor wind temperature is over 28°C. Case study-2 is the suitable for windy regions.

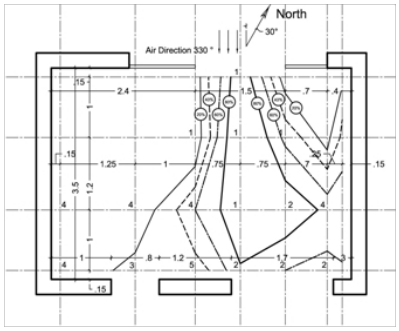

Architectural case study no-1

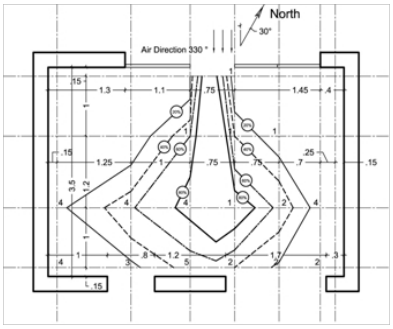

Architectural case study no-2

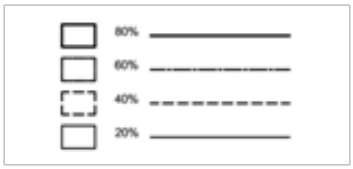

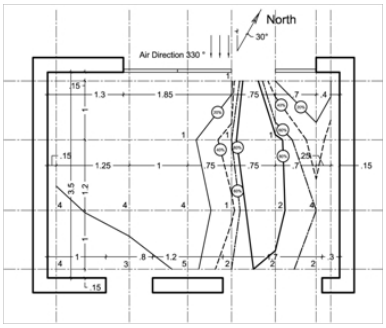

Architectural case study no-3

Figure (4): Effect of the ratio of inlet to outlet opening widths on indoor air velocity inside the room space model (for outdoor wind temperature 28°C, velocity 5 m/s and relative humidity 50%)

Table 4: Effect of the ratio of inlet to outlet opening widths on indoor air velocity inside the room space model (outdoor wind temperature 28℃, velocity 5m/s and relative humidity 50%)

Case studies	**The ratio between inlet opening& outlet opening Widths**	**The governing points for the inside air mass movement**					**Ventilation area for 20 % of wind velocity due to the total area**
		Point (1) air velocity at inlet opening	**Point (2) air velocity at primary outlet opening**	**Point (3) air velocity at secondary outlet opening**	**Point (4) air velocity at spread area**	**Point (5) air velocity at Stagnation wall**	
	Measurement units	**% of wind velocity**	**% of wind velocity**	**% of wind velocity**	**% of wind velocity**	**% of wind velocity**	**m^2**
Architectural case no.1	**2:3**	116	91	30	50	26-50	70%
Architectural case no.2	**1:3 Inlet opening facing wall**	150-165	40	10	60	50	65%
Architectural case no.3	**1:3 Inlet opening facing Outlet opening**	160-185	85	45	5-6	16	35%

Effect of outdoor wind velocity on cross ventilation

The effect of the outdoor wind velocity (4m/s - 7m/s) is presented in Figure (5) and Table (5). The lowest outdoor wind velocity case study -1 achieves the lowest values of the penetration points (1), (2) and (3), however, case study-1 increases the spread point (4) up to 70 % of outdoor wind velocity and the stagnation point (5) up to over 40 % and the covered ventilation area up to 61% of the total room space area. Therefore, the airflow rate in case study-1 has the lowest value to achieve only 1.45m^3/s. As a result, case study-1 is the suitable for high outdoor wind velocity regions resulted from stagnation effect. Meanwhile the highest outdoor wind velocity case study-4 achieves the highest values of the penetration points (1), (2) and (3), as a result, the airflow rate increases to nearly twice the previous case study value. The spread points (4) and (5) record the lowest values to equal only 20 %, as a result, the covered ventilation area of 20 % of outdoor wind velocity decreases to 54 %. Case study-4 is the suitable for low outdoor wind velocity regions resulted from the Venturi effect indoor velocity in case studies 2 and 3 that record average values for both air velocities and covered ventilation areas if compared to the previous two case studies. Case studies-2 and 3 are the suitable for both kinds of windy regions.

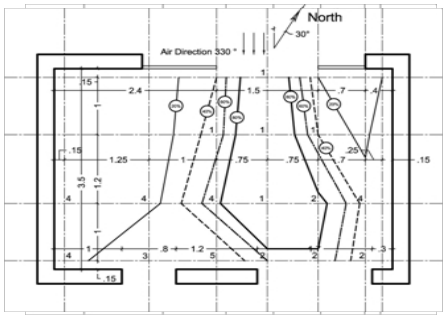

Velocity case study no-1

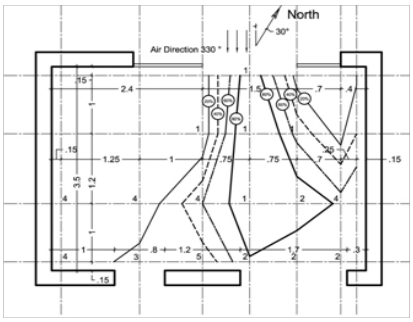

Velocity case study no-2

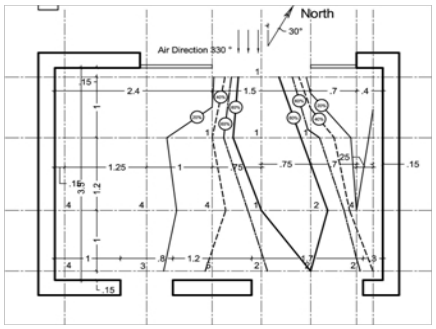

Velocity case study no-4

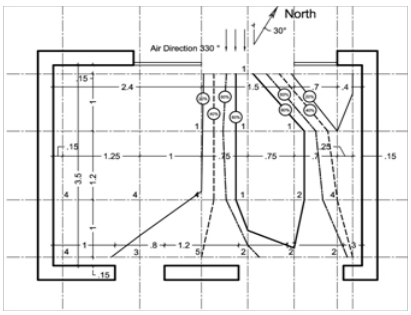

Velocity case study no-3

Figure (5): Effect of outdoor wind velocity on indoor air velocity inside the room space model (outdoor wind temperature 28°C and relative humidity 50%)

Table 5: Effect of outdoor wind velocity on indoor air velocity inside the room space model (outdoor wind temperature 28ºC and relative humidity 50%)

Case studies	Wind velocity	The governing points for inside air mass movements					Flow rate due to equations 1 and2	Ventilation area for 20 % of wind velocity due to total area	Estimated values of decreasing air temperature, [7]
		Point (1) Air velocity at Inlet opening	Point (2) Air velocity at Primary outlet opening	Point (3) Air velocity at Secondary outlet opening	Point (4) Air velocity at the Spreading area	Point (5) Air velocity at Stagnation wall			
Measurement units	**m/s**	**% of wind velocity**	**% of wind velocity**	**% of wind velocity**	**% of wind velocity**	**% of wind velocity**	**m^3/s**	**m^2**	**ºC**
Velocity case study no.1	4	92.5	50	36	77	46	0.4	61%	6
Velocity case study no.2	5	102.5	62.5	30	61	42	0.5	56%	7
Velocity case study no.3	6	105	67.5	27	28	30	0.6	54.65%	7.5
Velocity case study no.4	7	107.6	70	14	21.6	11.5	0.7	54.33%	8.25

Simulation results

Figures (6) and (7) present vectors of indoor air velocity. Tables (6) and (7) present indoor air velocity at the governing; the first three penetration points are at the openings while the other four spread points are at the facing wall and in the middle of the room space as shown in Figure (3).

Effect of the outdoor wind velocity on indoor cross ventilation in case study 1

Three wind velocity case studies 4 m/s, 6 m/s and 8 m/s with relative humidity 50 % are simulated as shown in Figure (6). Case study 1-1 can achieve the highest indoor covered ventilation area 50% of the total room space area that its indoor air velocity equals 2 m/s instead of 40% in case study 1-2 and 25% in case study 1-3.

Table (6) details both the stagnation and the Venturi effects at the governing points. The stagnation point (4) records 45% of outdoor wind velocity in the three case studies while the Venturi points record 90% of outdoor wind velocity in the three case studies; which means that the Venturi

effect achieved when the inlet opening faces the outlet opening is the suitable for low outdoor wind velocity less than 4 m/s.

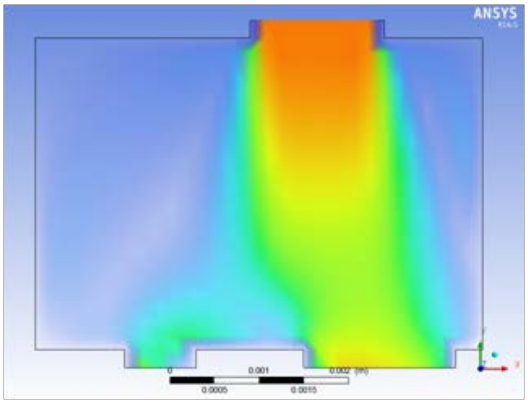

Case-1-1 Wind velocity 4 m/s
Relative humidity 50%

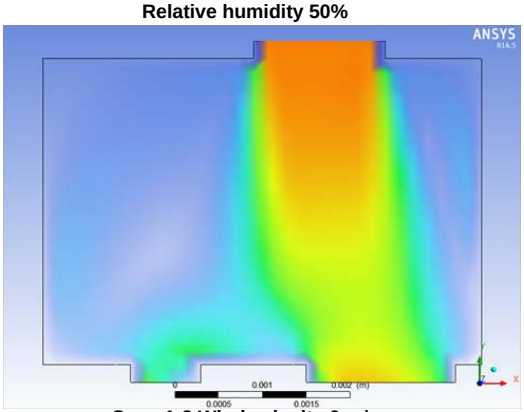

Case-1-2 Wind velocity 6 m/s
Relative humidity 50%

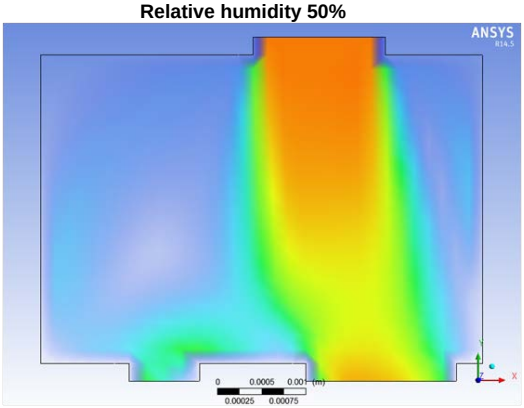

Case-1-3 Wind velocity 8 m/s
Relative humidity 50%

Figure (6): Effect of outdoor wind velocity on indoor air velocity inside the room space model (simulation experiments of the architectural case study no-1)

Table 6: Effect of outdoor wind velocity on indoor air velocity inside the room space model (simulation experiments of the architectural case study no-1)

Case	Case studies	Initial conditions	Governing points						
			1	2	3	4	5	6	7
Case 1	Case 1-1 V = 4 m/s RH=50 %	V m/s	4	4.06	3.80	1.55	4	1.55	0.350
		RH %	45	43	42.6	44	44	41	32
	Case 1-2 V=6m/s RH=50 %	V m/s	6	5.11	5.68	2.75	6.0	1.78	0.43
		RH %	50	.48	47	49.9	49.99	45	34
	Case1-3 V=8 m/s RH=50 %	V m/s	8	6.16	6.82	4.56	8.14	2.70	1.15
		RH %	50	50	49	50	50	46	30

2.2.2. EFFECT OF OUTDOOR WIND VELOCITY ON INDOOR CROSS VENTILATION IN CASE STUDY 2

Three outdoor wind velocity case studies 4 m/s, 6 m/s and 8 m/s with relative humidity 50 % are simulated as shown in Figure (7). Case study 2-1 can achieve the highest indoor covered ventilation area 35% of the total room space area that its indoor air velocity equals 2 m/s instead of 30% in case study 1-2 and 25% in case study 1-3.

Table (7) details both the stagnation and the Venturi effects at the governing points. The stagnation point (4) records 30% of outdoor wind velocity in the three case studies while the Venturi points record 70% according to wind velocity in the three case studies 1-1, 1-2 and 1-3. Table (7) explains how case study 2 with its different outdoor wind velocities achieves a high performance of cross ventilation in spite of both the high outdoor wind velocity and the narrow width of the inlet opening that increases uncomfortably the indoor air velocity. Because the facing wall due to the inlet opening can achieve the stagnation condition by decreasing the outdoor wind velocity by 70%; case study 2 is the suitable for high outdoor wind velocity more than 4 m/s.

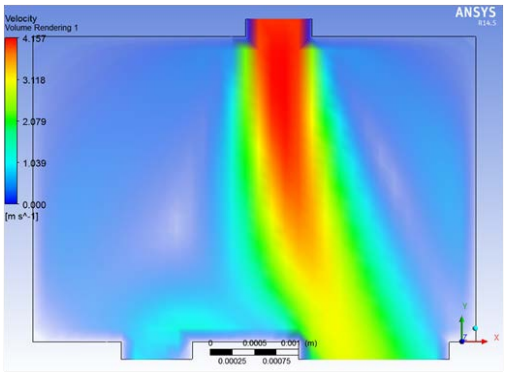

Case 2-1 Wind velocity 4 m/s
Relative humidity 50%

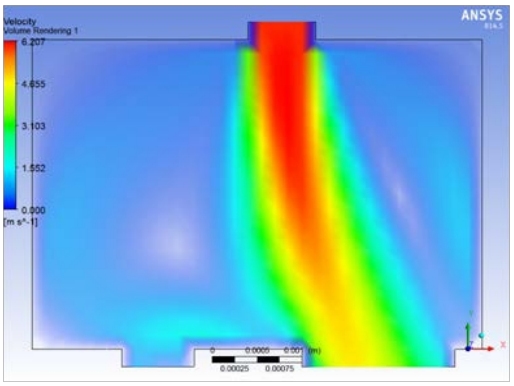

Case 2-2 Wind velocity 6 m/s
Relative humidity 50%

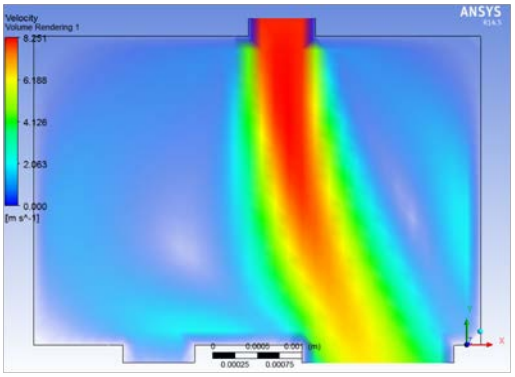

Case 2-3 Wind velocity 8 m/s
Relative humidity 50%

Figure (7): Effect of outdoor wind velocity on indoor air velocity inside the room space model (simulation experiments of architectural case study no-2)

Table 7: Effect of outdoor wind velocity on indoor air velocity inside the room space model (simulation experiments of the architectural case study no-2)

Case	Case studies	Initial conditions	Governing points						
			1	2	3	4	5	6	7
Case2	Case 2-1 V = 4 m/s RH=50 %	V m/s	4.0	1.40	2.98	1.25	4.23	0.60	1.40
		RH %	0.50	0.37	0.445	0.478	0.4999	0.27	0.36
	Case 2-2 V=6m/s RH=50 %	V m/s	6.0	2.21	4.50	2.05	6.02	0.80	1.20
		RH %	0.50	0.37	0.45	0.478	0.4999	0.27	0.32
	Case2-3 V=8 m/s RH=50 %	V m/s	8.0	2.84	6.0	2.26	8.4	0.88	0.97
		RH %	0.50	0.31	0.45	0.478	0.499	0.27	0.34

VALIDATION RESULTS

Table (8) presents the differences between field and simulation measurement values in percentages of outdoor wind velocities. Case study 1 as shown in Figures (1) and (2) is validated. The governing points at the openings and the facing walls across the five horizontal grid lines due to windward side are validated. The average differences between field and simulation measurements are(±20%) because of the instability of the actual outdoor wind velocity.

Table 8: Validation between field and simulation results

Case study number	Type of measurement& The difference between them Values % of wind velocity	Inlet opening								Left outlet opening				Right outlet opening			Stagnation point	
		Center				Corner												
		horizontal	1 m	2 m	3 m	0 m	1 m	2 m	3 m	0 m	1 m	2 m	3 m	1 m	2 m	3 m	2 m	3 m
Case no.1 velocity 4 m/s	Field	128	128	128	64	69	37	90	77	19.2	37	90	77	4	13	36	77	11
	Ansys	100	101	99.5	78.25	54	78	77	70	54.1	78	70	70	16	24	47	74	45
	Difference	28	27	28	14	15	40	12	7	35	40	20	7	12	11	11	3	34
Case no.2 velocity 6 m/s	Field	103	113	95	76	19	56.6	95	56.6	103.7	113	95	75	15	10	30	60	30
	Ansys	100	102.7	101	85	100	100	160	73	100	100	95	73	31	25	13.5	66	72.3
	Difference	3.7	11	6	10	81	46	5	16	3.7	13	6	2	16	15	17	6	42
Case no.3 velocity 6m/s	Field	96	112	112	60	12.5	104	96	75	96	112	96	75	6.4	14	27	21	40
	Ansys	100	102.5	103	85	100	100	95	100	100	100	100	101	31	23	90	12	90
	Difference	4	10	9	25	88	4	1	25	4	12	4	26	15	9	63	9	40

Discussions and recommendations

- The stagnation condition inside the indoor single room space model occurs when the inlet opening faces the walls meanwhile the Venturi condition inside the indoor single room space model occurs when the inlet opening faces the outlet opening.

- The shapes of the indoor continuous contour lines that are ratios of the outdoor wind velocity indicate the stagnation or the Venturi conditions where the curve shapes of the contour lines result from increasing the spread points at the facing walls meanwhile the spire shapes of the contour lines result from increasing the penetration points at the openings. The curve shapes of the contour lines indicate the stagnation condition meanwhile the spire shapes of the contour lines indicate the Venturi condition.

- In windy regions, the favorite stagnation and Venturi effect case studies are to achieve the appropriate air velocities with a maximum indoor covered ventilation area of air mass movements inside the indoor room single space model. as possible.

- The stagnation effect can decrease the outdoor wind velocity from 55% to 70% meanwhile the Venturi effect can increase outdoor wind velocity from 70% to 150% in tested model.

- Many factors can be obtained from the results related to the architectural design decisions to improve the tested single room space model by suggesting the modified model that can achieve thermal comfort for the different outdoor wind velocities to be the suitable to a windy region.

SUGGESTED MODELS DUE TO OUTDOOR WIND VELOCITY

Two suggested types of models are designed in accordance with the stagnation and the Venturi effects .The suggested models are based on both the high outdoor wind velocities as the first priority and the moderate outdoor wind velocities due to Beafaurt scale [13] as the second priority. The indoor dimensions of the first model are more than the tested previous model in the length of the room space to decrease air velocities. The stagnation effect can be achieved in the suggested models architecturally. The dimensions of the two models are the same as shown in Figure (8) with the only difference is that the first model has one inlet opening and two outlet openings meanwhile the second model has two inlet openings and one outlet opening. The first model indicates the stagnation effect while the second model indicates the Venturi effect.

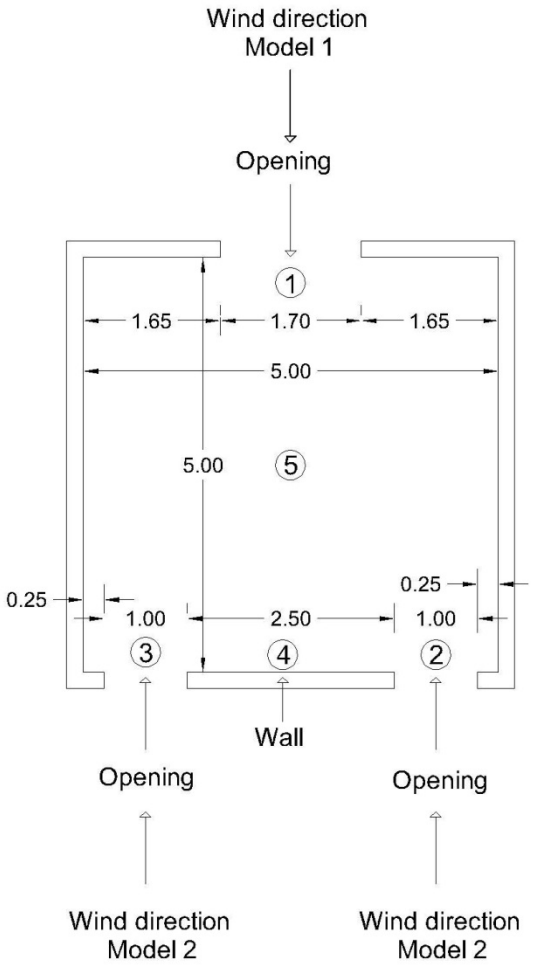

Figure (8); Description of the two suggested models with the indoor governing points

Simulation experiment results of the suggested models

The three outdoor wind velocities 4m/s, 6m/s and 8m/s are tested for the two suggested models. Case studies 1 and 4 are simulated for the outdoor wind velocity 4m/s. Case studies 2 and 5 are simulated for the outdoor wind velocity 6m/s .Case studies 3 and 6 are simulated for the outdoor wind velocity 8m/s.

Results of model one

Case studies 1, 2 and 3 of Figure (9) show the simulation experiments based on the different outdoor wind velocities 4 m/s, 6 m/s and 8 m/s. Maximizing the stagnation effect and minimizing the Venturi effect are required. The curve shapes of air velocity contour lines are formed; the shapes indicate the increase of both the stagnation effect and covered

ventilation areas. Case study 1 can achieve the average indoor air velocity 2.2 m/s; this value can achieve thermal comfort. Case study 2 can achieve the average indoor air velocity 3.35 m/s in spite of the higher outdoor wind velocity 6m/s; this case study can decrease the indoor air velocity to 2m/s in the human activity area to achieve the acceptable value due to thermal comfort. Case study 3 can achieve the average indoor air velocity 4.35 m/s in spite of the highest outdoor wind velocity 8m/s; this case can decrease the indoor air velocity to 3.48 m/s in the human activity area to achieve the acceptable value due to thermal comfort.

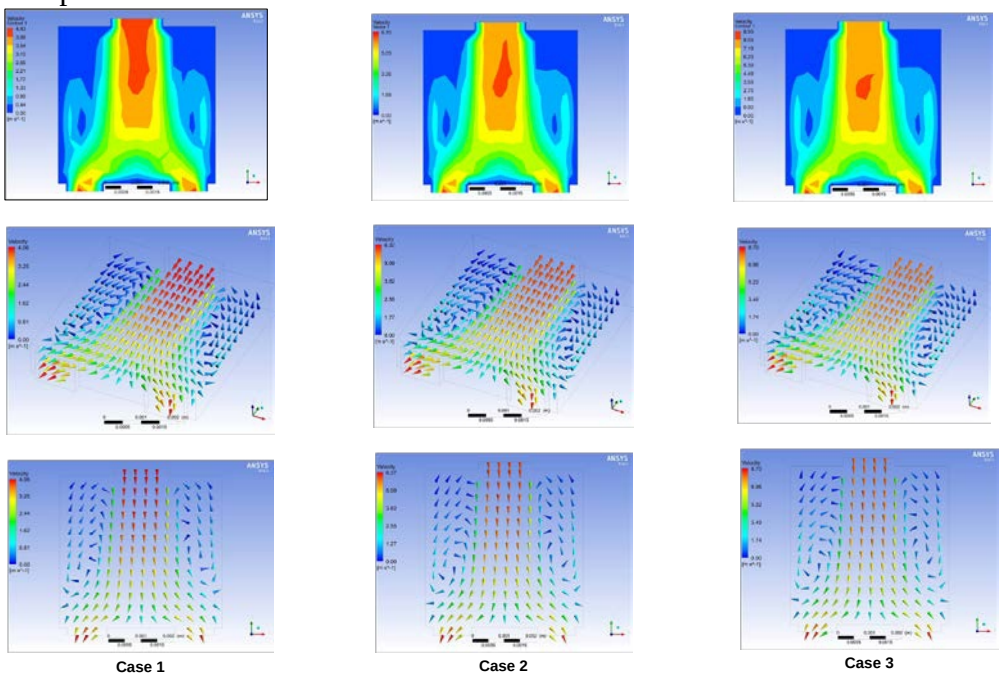

Figure (9) Simulation experiments for the suggested model one

Results of model two

Case studies 4, 5 and 6 of Figure (10) show the simulation experiments based on the different outdoor wind velocities 4 m/s, 6 m/s and 8 m/s. Maximizing the Venturi effect and minimizing the stagnation effect are required. The spire shapes of air velocity contour lines are formed; the shapes indicate the increase of both the Venturi effect and air flow rates. Case study 4 can achieve the average indoor air velocity 3.25 m/s; this value is higher than that in case 1 that has the same outdoor wind velocity. In spite of the higher average indoor air velocity for both case studies 5 and 6 that ranges between 5m/s to 7m/s , the distance between the two inlet openings creates the favorite indoor zone due to the comfortable air velocity . Indoor

air velocity in the human activity area ranges between 3m/s to 4m/s; these values are acceptable due to thermal comfort.

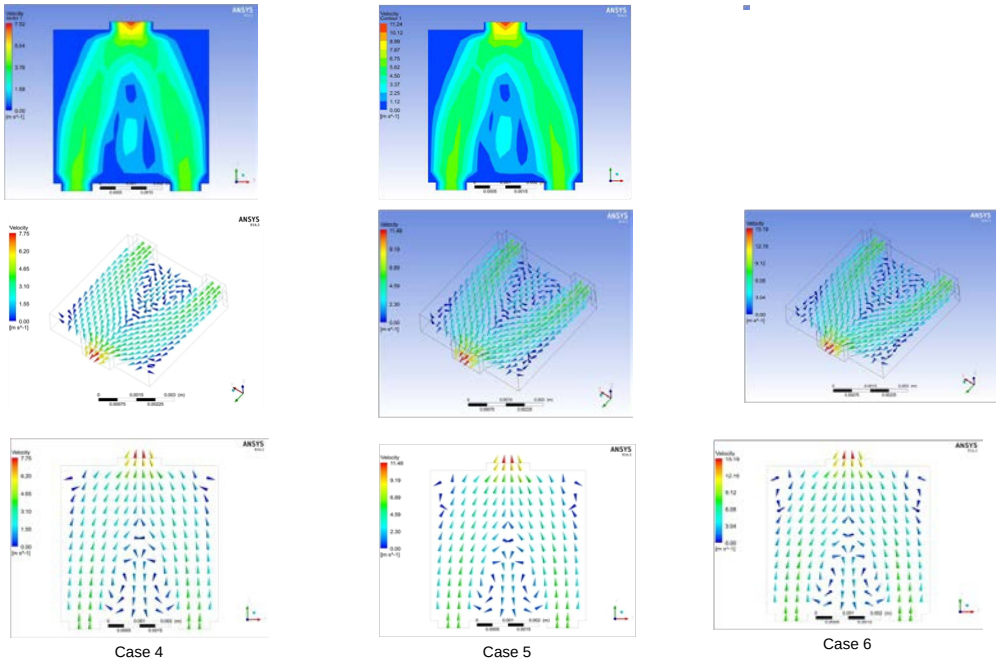

Figure (10) Simulation experiments for the suggested model two

Comparative studies

Comparative study between the two models:

Table (9) presents the ratios of the governing points due to the values of the outdoor wind velocities 4m/s , 6 m/s and 8m/s .

In the first suggested model, the model can achieve comfortable indoor air velocities in spite of the high outdoor wind velocities. The model can decrease outdoor wind velocities to 40% in indoor covered ventilation areas 60% of the room space total areas. Indoor air velocities at the openings equal outdoor wind velocities. The condition is acceptable for high outdoor wind velocities.

In the second suggested model, the model can achieve acceptable indoor air velocities in spite of the highest outdoor wind velocities. The model can increase indoor air velocities at the openings around twice outdoor wind velocities. But this model can decrease indoor air velocities to around 65% of outdoor wind velocities in the middle of the room space. Commonly, the condition is the favorite for low outdoor wind velocities.

Table (9) Comparative study between the two suggested simulated models

Number of the model	Wind velocity	Governing points (ratios of the wind velocity)				
		1	2	3	4	5
First model	4m/s	110%	99.5%	99.5%	90%	33.25%
	6m/s	92%	88%	88%	96%	31%
	8m/s	100%	88%	88%	96%	33-62%
	Average	100%	90%	90%	94%	40%
Evaluation of the first model		Suitable for high wind velocities				
Second model	4m/s	175%	95%	95%	60-75%	25%
	6m/s	175%	95%	95%	75%	25-30%
	8m/s	175%	112.5%	112.5%	50%	27.5-37%
	Average	175%	100%	100%	60%	30%
Evaluation of the second model		Suitable for low wind velocities			Suitable for high wind velocities	

Comparative study between field and suggested simulated models

In the stagnation effect condition, the curve shapes of the contour lines indicate the ratio of outdoor wind velocities formed in both the field and the suggested simulated models as shown in Figure (11). Velocity case study 1 and the architectural case study 2 of the field models have similar shapes of the contour lines of the suggested simulated model one as shown in Figure (11).

Meanwhile in the Venturi effect condition, the spire shapes of the contour lines indicate the ratio of outdoor wind velocities formed in both the field and the suggested simulated models as shown in Figure (12). Velocity case study 4 of the field models has similar shapes of the contour lines of the suggested simulated model two as shown in Figure (12).

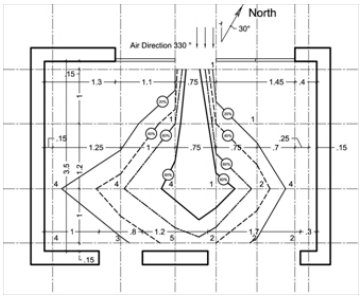

Architectural case study no-2 wind velocity 6 m/s

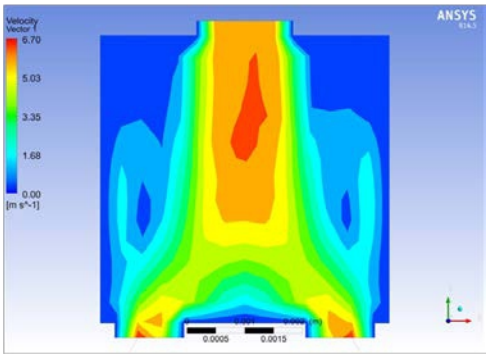

Suggested model 1 case study no-2 wind velocity 6 m/s

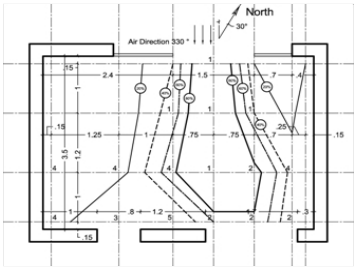

Velocity case study no-1 wind velocity 4 m/s

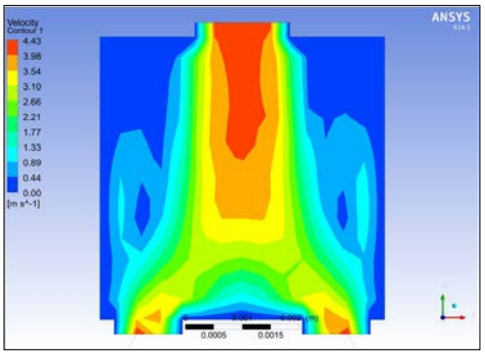

Suggested model 1 case study no-1 wind velocity 4 m/s

Figure (11) Comparative study between field and suggested simulated models in the stagnation condition

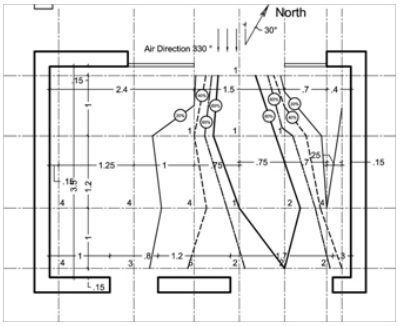

Velocity case study no-4 wind velocity 8 m/s

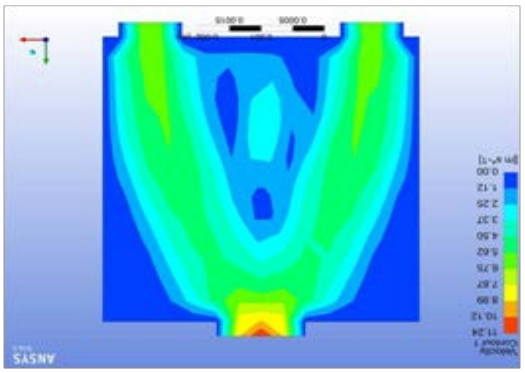

Suggested model 2 case study no-3

Figure (12) Comparative study between field and suggested simulated models in the Venturi condition

Conclusion

The stagnation effect can be applied when the outdoor wind velocity equals or is more than 4 m/s meanwhile the Venturi effect can be applied when the outdoor wind velocity equals or is less than 4 m/s.

References:

Givoni, B., Passive and low energy cooling of buildings, Van Nostrand Reinhold, 1994, New York.

Borger, G.S. and De Gear,R., A standard for natural ventilation, ASHREA Journal, October 2000: 21-28.

Givoni, B. Man, Climate and architecture, Applied science publishers, 1969, London.

Olgyay, V. Design with climate, Princeton university press, 1963.

ASHRAE fundamentals handbook, ASHRAE (American Society of Heating, Refrigerating and Air-Conditioning Engineers), 2005, Atlanta, GA.

Karava,P., Stathopoulous, T. and Athienitis,A.K., Airflow assessment in cross- ventilated buildings with operable façade elements, Building and environment 46, 2011, p.p. 266-273.

Abdin,A., A bio-climatic approach to house for semi-desert and hot climates with special reference to Egypt, Department of architecture building science, University of Strathclyde, Galascow, 1982.

Anderson,J.D., Fundamentals of aerodynamics, McGrow-Hill book company,1984.

Allard,F., Bastide, A. and Boyer,H., Natural ventilation: A new method based on Walton model applied to cross-ventilated buildings having two large openings, Nordic Journal of building physics, Vol.2, 1999.

Mass,A., Experimental and theoretical case study on cross ventilation-designing a mathematical model, Nordic Journal of building physics, 1999.

EMA (Egyptian Meteorology Authority), 2013, Cairo, Egypt.

Energy Plus (Energy simulation software), Weather data, 2013.

Southampton weather, Hampshire, United Kingdom, 2014.